Journal of Radiological Protection

Official journal of the Society for Radiological Protection

REVIEW • OPEN ACCESS

Review of x-ray exposure and safety issues arising from ultra-short pulse laser material processing

To cite this article: Herbert Legall *et al* 2021 *J. Radiol. Prot.* **41** R28

OPEN ACCESS
IOP Publishing | Society for Radiological Protection Journal of Radiological Protection
J. Radiol. Prot. **41** (2021) R28–R42 (15pp) https://doi.org/10.1088/1361-6498/abcb16

Review

Review of x-ray exposure and safety issues arising from ultra-short pulse laser material processing

Herbert Legall, Jörn Bonse and Jörg Krüger

Bundesanstalt für Materialforschung und -prüfung (BAM), Unter den Eichen 87, Berlin D-12205, Germany

E-mail: herbert.legall@bam.de

Received 7 September 2020; revised 12 November 2020
Accepted for publication 17 November 2020
Published 26 February 2021

Abstract

Laser processing with ultra-short laser pulses enables machining of materials with high accuracy and throughput. The development of novel laser technologies with laser pulse repetition rates up to the MHz range opened the way for industrial manufacturing processes. From a radiological point of view this evolution is important, because x-ray radiation can be generated as an unwanted side effect in laser material processing. Even if the emitted x-ray dose per pulse is comparably low, the x-ray dose can become hazardous to health at high laser repetition rates. Therefore, radiation protection must be considered. This article provides an overview on the generation and detection of x-rays in laser material processing, as well as on the handling of this radiation risk in the framework of radiological protection.

Keywords: ultra-short pulse laser processing, laser-induced x-ray emission, radiation protection

(Some figures may appear in colour only in the online journal)

1. Introduction

The advantages of contactless material processing with laser beams are manifold regarding precision of surface contours, productivity, potential automatisation and high reproducibility and versatility. These advantages must overcompensate the high investment and maintenance

costs in laser material processing. However, the productivity can only be increased to a certain limit without losing the precision in the machining process. Precision is lost at high thermal input by melt formation. For ultra-short laser pulses with durations <10 ps and a proper choice of processing parameters, the amount of melt can be reduced and nearly avoided [1]. Laser technologies providing laser repetition rates in the kHz to MHz range along with pulse durations ranging from femtoseconds to picoseconds and laser pulse energies in the >μJ range [2–4], allow for an efficient treatment of material. Typical ultra-short laser machining processes are the laser surface ablation with structuring down to the 100 nm range (e.g. for the realization of functional surfaces), the laser drilling of holes and grooves with dimensions down to a few micrometres, fine laser cutting and a force- and deformation-free micrometre range laser-assisted turning.

In the late 1980s it was already shown that during ultra-short sub-ps pulse laser material interaction x-ray radiation can be produced [5–9]. The aim of these early studies was the production of ultra-short x-ray pulses mostly under vacuum conditions. One decade later, Thogersen *et al* reported on x-ray emission during femtosecond laser micromachining in air. Using 120 fs laser pulses with kHz repetition rate and laser pulse energies of maximal 280 μJ, the authors stated that laser treatment of copper resulted in high x-ray dose rates and a radiation shielding of the apparatus is necessary. Additionally, it was suggested that x-ray radiation can be used as a monitoring tool for laser processing [10]. For the kHz repetition rate range, Bunte *et al* confirmed that the laser-matter interaction of tightly focused sub-mJ femtosecond laser pulses in air can cause x-ray radiation levels close or even above the regulatory radiation limits for the public [11]. With the availability of laser sources suitable for industrial use having repetition rates in the several 100 kHz to MHz range, new investigations on harmful x-ray emissions became more and more urgent. In recent years several groups started to work on this topic and published first results [12–17]. The status of the work is presented here in an overview.

2. Ultra-short pulse laser material processing

2.1. The laser ablation process

Laser processing of solids by ultra-short laser pulses can be divided in three stages:

(a) In a first step, the laser radiation is absorbed by the electronic system of the solid and may be redistributed within it. Depending on optical properties of the solid, the deposition of optical energy occurs during the laser pulse and can involve linear or nonlinear absorption processes. Additionally, ultrafast carrier–carrier scattering, free-carrier absorption (inverse Bremsstrahlung), avalanche ionization, or resonant coupling effects can contribute if a critical electron-plasma density is exceeded allowing the plasma electrons to act collectively.

(b) In the second step, the energy is transferred from the electronic system to the lattice of the solid. This occurs via electron–phonon scattering processes, typically on the timescales of a few hundreds of femtoseconds up to several picoseconds, depending on the material [1]. During the electron–phonon-relaxation time, the deposited optical energy stays locally confined as it cannot spread (yet) to the surrounding via heat diffusion. This energy confinement finally accounts for the high machining precision and for the small heat-affected zone that can be achieved with ultra-short laser pulses [18].

(c) In a third step, a permanent material modification is imposed if material and process specific energy density thresholds (e.g. oxidation, melting or ablation) are locally exceeded. The most widely used process of ablation may set on after some tens of picoseconds [19] and can last up to hundreds of microseconds. During this stage, neutral or charged atoms,

molecules, clusters, or particles are removed from the surface through an 'ablation plasma' that may even optically screen the surface from successive laser pulses ('plasma shielding') emitted at repetition rates larger than some hundreds of kilohertz.

In practice, laser processing is realized by focusing the laser radiation onto the sample surface by means of lenses, mirrors, axicons, or diffractive optical elements. The focused pulsed laser beam is applied to the surface either 'statically' (exploiting a certain number of pulses at a given pulse repetition frequency, e.g. for drilling of boreholes) or 'dynamically' if the beam is moved relatively to the surface allowing to control the scanning velocity. The latter scanning parameter defines the distance of neighboured irradiated spots. Upon moving the focused laser beam in a meandering way across the surface, large sample areas can be homogeneously treated. A 3D contour-shaping of the sample surface can be realized by combining defined sequences and repetitions of static or scan processing strategies.

Apart from the different spatial laser processing strategies, other laser machining parameters may be tailored for optimizing the laser processing duration or the final surface quality. The material removal (ablation) rate is affected by the average number of pulses per beam spot area (controlled by the scan velocity and the pulse repetition rate) and also by the applied peak intensity (controlled via the single laser pulse energy).

For higher productivity, the laser processing can be temporally sectioned into several successive machining steps. In these cases, often a pre-machining step is added to the process in which 'superfluous' material is removed at high ablation rates (pulse energies), while the required surface quality is subsequently achieved in a surface finishing step at small ablation rates. This combination of laser processing at high and low ablation rates is referred to as 'roughing and finishing' in the literature [20]. Particularly during the roughing step at high laser pulse energies, the emission of x-ray radiation in the keV range may occur.

2.2. Laser systems

Figure 1 shows pulse energies and repetition rates of existing laser systems (filled circles) in a double-logarithmic plot. Obviously, even on the 100 MHz repetition rate level, pulse energies exceeding the μJ range were realized. Average power laser systems providing >1 kW are available. In order to handle the high thermal input in the laser medium during the generation process of the laser pulse, technologies were developed, which allow for an efficient cooling of the laser medium, as the thin disk laser technology [2], the Inno-Slab technology [3] and the ultra-short pulse laser fibre technology [4]. Different configurations are offered by the laser manufacturers and can be bought already 'off-the-shelf'.

The most widely used ultra-short laser material processing machines today deliver pulses with durations between several 100 fs up to several ps, pulse repetition rates between several 100 kHz up to several MHz, and pulse energies from several μJ up to several mJ, yielding a total average power level of a few 10–100 W. For such laser systems, x-ray measurements were performed during laser materials processing and indicated with white filled circles in figure 1.

With several 100 W laser power and repetition rates in the MHz range, the heat introduced into the workpiece during the machining process is currently a limiting factor, as heat accumulation can lead to a reduced machining quality. Therefore, ultra-short pulse lasers in the kW range are not yet used in industrial practice. Smart heat management concepts are required for high repetition rate laser systems. Possible approaches include parallel processing technologies [22], the use of very fast polygon scanners [23], or a fast mechanical supported exchange of the material surface, like for example in the case of laser turning.

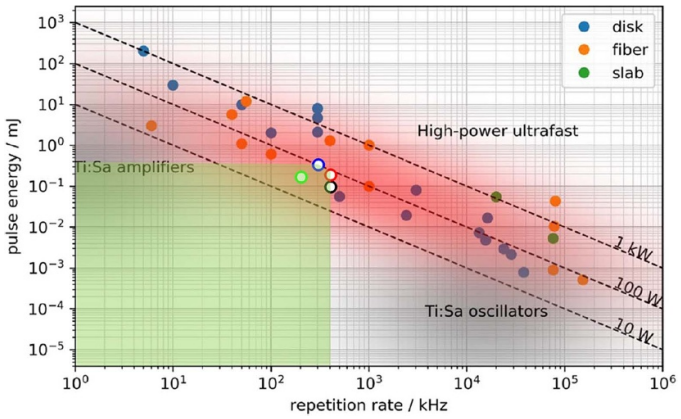

Figure 1. Overview of state-of-the-art ultrafast laser systems, based on different technologies (colour coded: disk, fibre, slab laser; see insert), illustrating the trend of current ultrafast laser technology towards multi-kilowatt average power [21]. In addition, the upper limit of laser pulse energy and repetition rate (covering the green area of laser parameters) were marked (white filled circles with collared outlines: black [12], red [13], blue [16], green [17]) for which the x-ray emission was investigated in laser material processing. Copyright 2019 under Creative Commons BY 4.0 license [21]. Retrieved from https://jeos.springeropen.com/articles/10.1186/s41476-019-0108-1.

3. Instrumentation

The detectors that can be used for radiation measurement in ultra-short pulse laser processing must be suitable for the generated pulsed x-ray radiation field. It should be noted that the temporal profile of the x-ray radiation field almost follows the temporal course of the laser pulse. Very small single pulse doses in the pSv to nSv range are generated with laser pulse repetition frequencies in the kHz to GHz region. In addition, the radiation detector should not have dead times that could lead to an underestimation of the total dose. Furthermore, the emitted radiation field in laser material processing cannot be regarded as quasi-continuous radiation field with a constant averaged dose level since the strength of the emitted radiation field can change substantially during the machining process. The dynamic range of the detectors must therefore be large enough to detect the low single pulse doses (laser finishing step) as well as high peak doses (roughing step) in the micro-machining process. As will be shown in a later section, the generated x-ray dose scales nonlinear with the incident laser pulse energy. The complexity of the choice of a general suitable measuring instrument from the perspective of radiation protection is thus motivated by the great variety of laser and processing parameters potentially applied in laser machining. In the following, the available instrumentation will be presented and discussed with regard to its suitability for radiation measurements in ultra-short pulse laser material processing, after a short introduction to the measurable radiological quantities.

3.1. Quantities in radiological protection

'Protection quantities' were introduced for risk assessment of human exposure to x-ray radiation and for the determination of personal dose limits in radiological protection by the International Commission on Radiological Protection (ICRP) [24]. The human body-related and not directly measurable protection quantities allow a quantification of the detriment to people from

exposure to ionizing radiation. The protection quantities for external x-ray exposure comprise the 'effective dose' for the whole-body and 'organ equivalent doses' for partial-body exposure. For use in radiation measurements the International Commission on Radiation Units and Measurements (ICRU) developed a set of 'operational quantities' as measurable surrogates. These quantities were defined by x-ray dose equivalents measured at a certain depth d of a standardized phantom, a tissue equivalent sphere (ICRU-sphere), e.g. the dose equivalent measured at a depth of 10 mm of the ICRU-sphere corresponds to the effective dose and the dose equivalent measured at 0.07 mm depth corresponds to the skin dose. The operational quantities are subdivided in ambient dose equivalents $H^*(d)$, in directional dose equivalents $H'(d,\Omega)$ and in personal dose equivalents $H_p(d)$. Herein, the quantity Ω denotes the angle of incidence of the x-ray radiation to the ICRU-sphere. While ambient and directional dose equivalents are used to control the area exposure, personal dose equivalents monitor the exposure dose of an individual. For members of the public the ICRP recommended a dose limit of 1 mSv a^{-1} for the effective dose and 50 mSv a^{-1} for the exposure of the skin [24]. The dose limits were adopted by most countries. Dose limits for working personal must be related to the occupational exposure time per year. The regulatory radiation limits for working personal can differ from country to country.

In practice the 'protection quantities' and 'operational quantities' are related to basic measurable 'physical quantities', as e.g. the fluence, the absorbed dose or the air kerma. Conversion coefficients provided by the ICRP are used for the calculation of the x-ray doses from these physical quantities.

3.2. Instrumentation for monitoring the x-ray dose

Concerning the temporal characteristics of the emitted x-ray radiation field, an ultra-short pulse laser material processing system can be best compared to common x-ray flash units. Here, guidelines apply according to which the determination of the ambient x-ray dose should be performed preferably with dose storing passive dosimeters. If no adequate dosimeters are available for certain dose measuring purposes, the authorities may permit the use of other instrumentation in individual cases. Since passive dosimeters must be read out manually after an exposure, this dosimeter type is not convenient in practical use if measurements must be repeated many times, e.g. for the alignment of a radiation source. For monitoring the emitted x-ray radiation dose active dosimeters are more useful. However, there are some restrictions in the use of active dosimeters in pulsed radiation fields [25]. Counting dosimeters (counter tubes, scintillators), for example, show too low doses in pulsed radiation fields due to the intrinsic dead times [26]. A selection of electronic personal dosimeters was approved up to a certain pulse dose limit for x-ray diagnostics in medicine with pulsed radiation typically in the ms range. However, at shorter pulse durations with higher peak doses the response sensitivity of these dosimeters decreases, which can lead to an underestimation of the x-ray dose [27]. Currently, no 'authorized' recommendation for a specific dosimeter type for the measurements in ultra-short laser material processing is available.

So far ionization chambers were used in most measurements of the x-ray radiation field emitted in laser material processing. These instruments are characterized by high detection sensitivity and can be equipped with a sufficiently large chamber volume to prevent saturation losses due to high peak doses. In [12] an ionization chamber was proven for x-ray measurements in ultra-short pulse laser material processing. The verification was performed by comparing the simultaneously accumulated x-ray doses collected with a passive dosimeter with direct ion storage (DIS-1, Mirion Technologies GmbH) and an air-open ionization chamber (OD-02, STEP GmbH). In this comparison it was assumed that in the considered energy range

the personal dose $H_p(0.07)$ (and $H_p(10)$) measured with the passive dosimeter at an incidence angle of 0° can be set equal to the directional (and ambient) equivalent dose $H'(0.07)$ (and $H^*(10)$) up to a photon energy range of 50 keV [28]. For the measurements, the ionization chamber was operated in a mode in which the chamber current was accumulated by charging a capacitor. The capacitor voltage can be related to the corresponding dose of the pulse at the end of the electrical charging process. The comparison revealed a linear dependence with a slope of 1 between the accumulated directional equivalent dose $H'(0.07)$ collected by the OD-02 and the accumulated personal dose $H_p(0.07)$ collected by the passive dosimeter DIS-1. The averaged dose per pulse in these measurements was specified with 0.1 nSv at a laser pulse energy of 100 μJ, a laser pulse duration of 925 fs and a laser pulse repetition rate of 400 kHz [12].

3.3. Alternative instrumentation for x-ray measurements

In this section alternative instrumentation for x-ray photon measurements will be discussed. This comprises highly sensitive, dose storing area detectors, as e.g. phosphor imaging plates [29] or charge coupled devices, as well as instruments for spectral x-ray photon measurements. Area detectors can be used for the detection of leakages of a radiation protection cabinet. The knowledge of the spectral x-ray emission is particularly important if an adequate radiation protection shielding is to be calculated. Instruments for the measurement of the spectral photon flux in pulsed radiation fields are e.g. efficient broadband x-ray crystal spectrometers combined with an area detector [30, 31], single photon counting semiconductor-based spectrometers [32] and thermo luminescence detector (TLD) -based few channel spectrometers [33]. Crystal spectrometers are restricted in the energy range and sensitivity to spatial variations of the source position. TLD-based few channel spectrometers are reliable in the measurement of pulsed x-ray radiation but highly complex in evaluation. Semiconductor-based spectrometers can cover a broad energy range, tolerate position changes of the x-ray radiation source, deliver the spectrum almost instantaneously and are easy to handle. The high stopping power of semiconductor detector materials, as e.g. CdTe provides a detection efficiency of almost 100% over a broad energy range. Even though these detectors are ideally suited for the measurement of pulsed radiation fields, this detector type has some disadvantages, e.g. its vulnerability to pile-up. This effect arises, if multiple x-ray photons hit the single photon detector in the time frame of the processing time and are registered as one single photon with higher energy. To minimize the pile-up, the spectrometer can be operated at a large distance to the x-ray radiation source and in addition, the emitted radiation can be attenuated by filters placed in front of the x-ray detector. The so far published spectral investigations of the x-ray emission from laser material processing at low single pulse doses with high laser pulse repetition rate were performed with a TLD-based few channel spectrometer [13, 33] and a CdTe-spectrometer (X-123, $3 \times 3 \times 1$ mm^3, 100 μm Be window, Amptek Inc.) [12, 16]. In figure 2, x-ray photon flux spectra evaluated from x-ray measurements with a CdTe-spectrometer (figure 2(a)) and a TLD-based few channel spectrometer (figure 2(b)) are presented. The measurements were performed under nearly identical laser processing conditions. At a distance of 100 mm to the radiation source, the evaluated photon numbers are comparable in both measurements.

4. The emitted x-ray radiation field

4.1. Factors influencing the emitted x-ray radiation field

The spectral distribution and intensity of the x-ray radiation field emitted in laser material processing depends on both, the laser and the processing parameters. The latter affect the

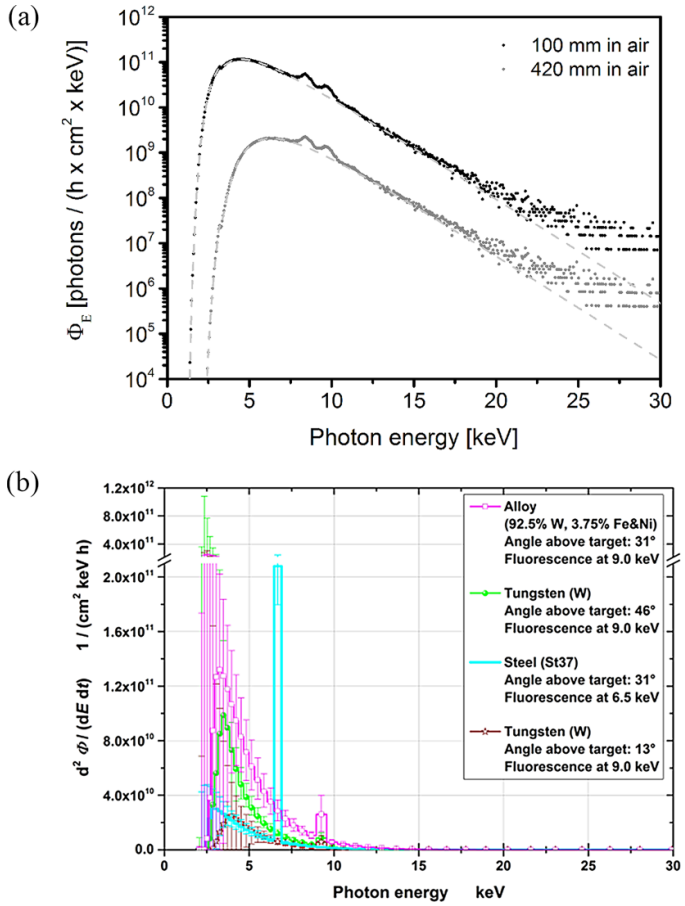

Figure 2. (a) The spectral x-ray photon flux Φ_E for tungsten calculated from measured spectra with a CdTe-spectrometer in air at an angle to the target surface of 29° and a peak intensity of 2.6×10^{14} W cm^{-2} at two distances to the ablation spot (100 and 420 mm) [12]. Additionally, the photon flux calculated from a Maxwell–Boltzmann distribution is shown (grey dashed line). Copyright 2018 under Creative Commons BY 4.0 license. Retrieved from https://link.springer.com/article/10.1007%2Fs00339-018-1828-6. (b) Flux spectra calculated from measurements in air at a peak intensity of 2.1×10^{14} W cm^{-2} performed with a TLD-based few channel spectrometer (normalized to the effective irradiation time and 100 mm distance) [13]. The uncertainty bars represent the 95% coverage intervals. Note that the ordinate is broken and has a ten times larger scale. The photon numbers of both spectra are comparable at a distance of 100 mm to the laser ablation spot. Copyright 2018 under Creative Commons BY 4.0 license. Retrieved from https://academic.oup.com/rpd/article/183/3/361/5090842.

surface topography and can lead to an increased thermal input into the material, which seems to favour the x-ray generation process [14]. Furthermore, as shown in figure 3 the dose rate of the emitted radiation field depends on the atomic number Z of the processed material [12, 16].

The upper graph (figure 3(a)) shows that the annual irradiation limit for the skin of 50 mSv can be reached after 1 h for laser treatment of tungsten and steel with peak intensities of the order of 10^{14} W cm^{-2}. The lower graph (figure 3(b)) visualizes the influence of the laser irradiation wavelengths by comparing the measurements for tungsten and steel for laser irradiation

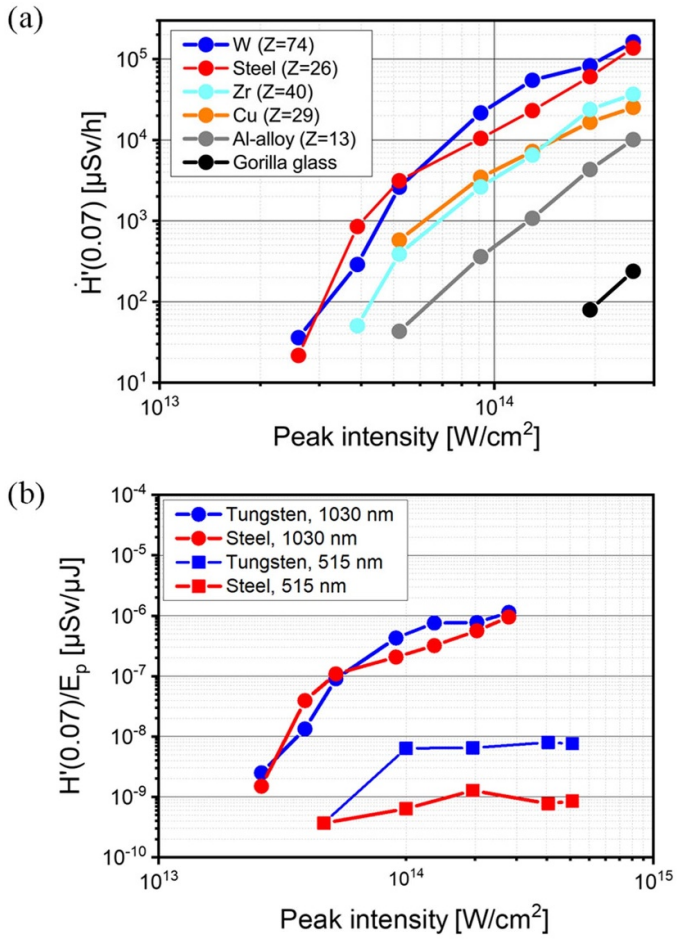

Figure 3. (a) Dose rates $\dot{H}'(0.07)$ in dependence on the material and the incident laser peak intensity at a laser wavelength of 1030 nm, an averaged laser power of 40 W, laser repetition rate of 400 kHz, a pulse duration of 925 fs and a focal spot diameter of 10 μm. Different target materials were investigated (tungsten, steel (S235JR), aluminium-alloy (AlMgSi0.5), zirconium, copper, and Gorilla glass) using the ionization chamber dosimeter OD-02 at a distance of 420 mm in air [16]. Reprinted with permission from (Legall H, Schwanke C, Bonse J and Krüger J 2020 *J. Laser Appl.* **32** 022004). Copyright 2020, Laser Institute of America. (b) Ratio of dose rate $\dot{H}'(0.07)$ and laser pulse energy E_p as a function of incident laser peak intensity derived from measurements with the OD-02 detector at a distance of 420 mm from the processing zone at a pulse duration of 925 fs, a repetition rate of 400 kHz and a laser wavelength of 1030 nm [16] and measurements at a distance of 200 mm, a pulse duration of 900 fs, a repetition rate of 20 kHz and a laser wavelength of 515 nm [17]. Both measurements were scaled to a distance of 420 mm without considering an absorption of x-ray radiation in air.

at 1030 nm [16] and 515 nm [17]. For a direct comparison, the dose was normalized by the laser pulse energy, taking into account different pulse repetition rates [16, 17]. Obviously, the ratio of dose per laser pulse energy at 515 nm is significantly lower than that at 1030 nm.

The spectral emission consists of continuous Bremsstrahlung and depending on the material of characteristic line emissions (cp. figure 2). The Bremsstrahlung spectrum follows a

Maxwell–Boltzmann distribution, where the characteristic parameter is the plasma electron temperature T_{hot} [12]. The direction of propagation of the emitted radiation field is spatially restricted by the local surface topography. The temporal response of the generated high energetic pulsed x-ray field follows almost the time envelop of the laser pulse [34]. In the following, the physical mechanisms which can lead to the generation of x-rays in the laser intensity range of about 10^{12}–10^{16} W cm^{-2} are presented and their dependencies on the applied laser and processing parameters are discussed.

4.2. Physical models and scaling laws

4.2.1. Physical models. In order to understand the process of x-ray generation in laser materials processing from a physical point of view, the currently known fundamental mechanisms which can lead to an x-ray generation in laser-plasma interaction must be considered [35–39]. In the intensity range between 10^{12}–10^{16} W cm^{-2} two mechanisms for the x-ray generation must be taken into account. Firstly, the plasma heating by 'collisional' absorption (inverse Bremsstrahlung), in which electrons distribute their kinetic energy absorbed from the laser radiation field through collisions with other electrons and ions in the plasma. Secondly, a mechanism in which the electric (laser) field resonantly excites plasma waves close to the surface of the over-dense plasma region, in which the laser field cannot propagate—a mechanism referred to as 'collision-less' absorption. It is commonly accepted, that at intensities below 10^{13} W cm^{-2} with a laser pulse duration in the ps–ns range, collisional absorption dominates the laser plasma interaction [35–39]. At intensities >10^{13} W cm^{-2} and shorter pulse durations in the femto- to picosecond range, however, collisional absorption loses its dominance, since the plasma has less time to expand and the volume in which the laser–plasma interaction can take place is strongly reduced. Therefore, in the intensity range between 10^{13}–10^{14} W cm^{-2}, collision-free absorption processes gain increasingly in importance. A collision-less absorption process that is known to be highly efficient in the intensity range $\geq 10^{15}$ W cm^{-2} is the so-called 'resonance absorption' [35–39]. The efficiency of this process depends on the plasma electron density gradient and the angle of incidence of the laser radiation onto the plasma surface. Furthermore, the electric field of the laser radiation must deliver a component along the plasma electron density gradient, i.e. the process depends strongly on the polarization state of the incident laser field [14]. For laser pulses with durations in the femtosecond region the plasma density gradient can become as steep that the coupling efficiency of the electric laser field to a resonant laser plasma oscillation diminishes. As a result, the efficiency of x-ray generation and thus the dose rates drop down for ultra-short laser pulse durations as depicted in figure 4. Here, for equal laser power, e.g. 10 GW, the emitted x-ray dose rate is the highest in the 6 ps case and the lowest for a pulse duration of 0.2 ps [40].

4.2.2. Scaling laws. The process of resonance absorption leads to a Maxwell–Boltzmann distribution of the spectral x-ray Bremsstrahlung emission, where the characteristic quantity for this distribution is the electron temperature T_{hot}. It could be shown, that this electron temperature scales with the intensity I of the laser pulse and laser wavelength λ as $(I\lambda^2)^{1/3}$, if all other parameters influencing the generation of Bremsstrahlung radiation are kept nearly constant [41].

Different scaling laws for the conversion of laser pulse energy in x-ray radiation energy were found. A scaling with $(E_{peak} \times Z)$ was proposed [42], where E_{peak} is the peak electric field of the laser pulse and Z is the atomic number of the target material. Using this scaling law, the conversion of laser pulse energy to x-ray is similar to the conversion law for conventional x-ray

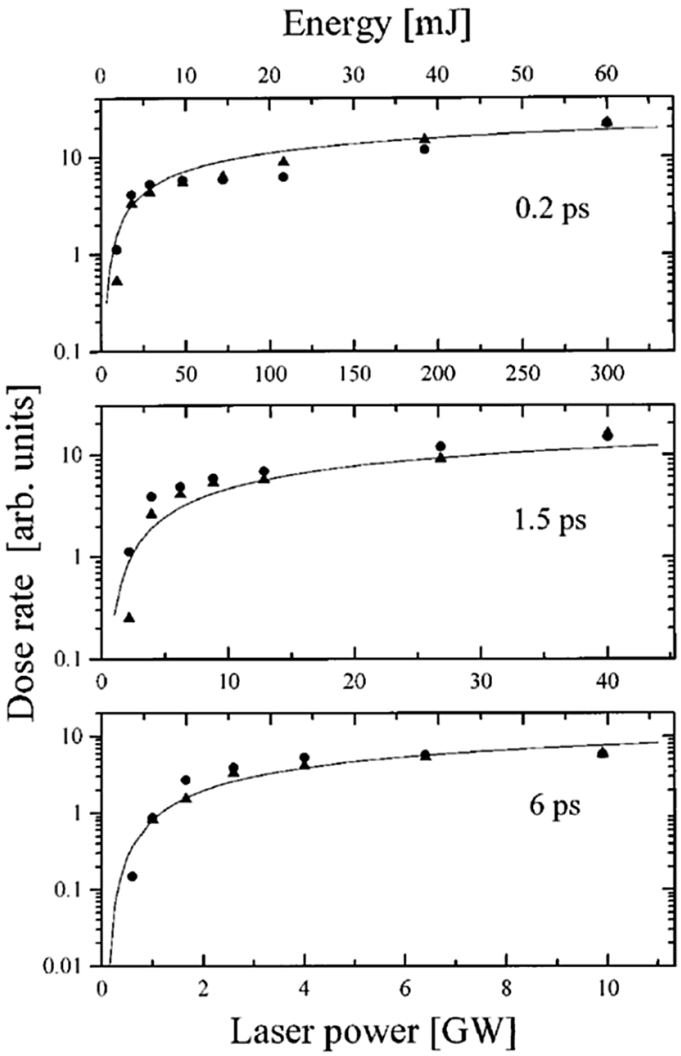

Figure 4. Dependencies of x-ray radiation dose rates for Cu and steel targets on the laser pulse power (laser pulse energy divided by laser pulse duration) for different pulse durations. Triangles are the dose rates for Cu and circles for steel targets. One arbitrary unit corresponds to 1 mSv h^{-1} [40]. Reprinted from (Chichkov B N, Momma C, Tünnermann A, Meyer S, Menzel T and Wellegehausen B 1996 *Appl. Phys. Lett.* **68** 2804), with the permission of AIP Publishing.

tubes, showing a scaling with the electron acceleration voltage and the atomic number of the target material. For the conversion of laser pulse energy (E) to x-ray Bremsstrahlung energy a dependence of ($Z \times E^2$) was proposed [43] which could be confirmed in measurements under laser material processing conditions [16].

Recently, an alternative scaling of the Bremsstrahlung emission was suggested by Weber *et al* [15]. Based on this model the dose rate in dependence on average laser power would scale with a power law as shown in figure 5. Utilizing an average laser power of 1 kW,

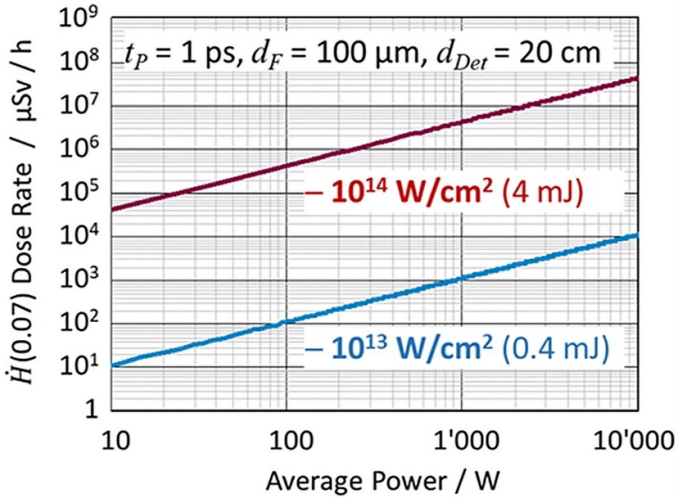

Figure 5. Expected dose rate $\dot{H}'(0.07)$ for tungsten at a distance of 200 mm as a function of the average laser power for a peak intensity of 10^{13} W cm^{-2} (blue line) and 10^{14} W cm^{-2} (red line) based on the model presented by Weber *et al* [15]. Copyright 2019 under Creative Commons BY 4.0 license. Retrieved from https://link.springer.com/article/10.1007/s00339-019-2885-1.

1 ps pulse duration and a peak intensity of 10^{14} W cm^{-2}, skin dose rates above 1 Sv h^{-1} are predicted for the treatment of tungsten.

5. Radiation protection

In this section the particular aspects of radiological protection in laser material processing and its implementation will be addressed.

5.1. Special aspects of radiological protection in laser material processing

As mentioned above, the emitted radiation field in ultra-short pulse laser material processing can best be compared with x-ray flash units. However, these two sources of x-ray radiation differ significantly in their spectral distribution of the emitted x-ray radiation field. While for x-ray tubes the emitted maximum spectral photon energy is determined by the applied acceleration voltage, for laser plasma radiation sources the photon flux in the keV range decreases exponentially with the x-ray photon energy in the tail of the Maxwell–Boltzmann distribution. Consequently, no maximum (specific limit) x-ray photon energy can be defined. Hence, the high-energy tail of the x-ray emission spectrum in laser material processing must be taken into account when calculating the shielding.

For investigations up to laser peak intensities of 2.6×10^{14} W cm^{-2} (400 kHz repetition rate, 925 fs laser pulse duration, 1030 nm laser wavelength), x-ray emission is limited to photon energies below 30 keV even for the treatment of tungsten [12, 13]. Here, a radiation protection shielding of 1 mm thick steel is suggested [12].

The dependence of the shielding efficiency of different potential protection materials on the photon energy was exemplarily calculated for photon energies of up to 60 keV [16]. It was shown that the attenuation of the x-ray radiation strongly decreases for photon energies

Table 1. Equivalent thickness of different shielding materials for x-ray protection up to photon energies of 60 keV in units of iron.

Material	Equivalent thickness (mm)
Iron	1
Aluminium	22
Borosilicate glass	40
Lead	0.5

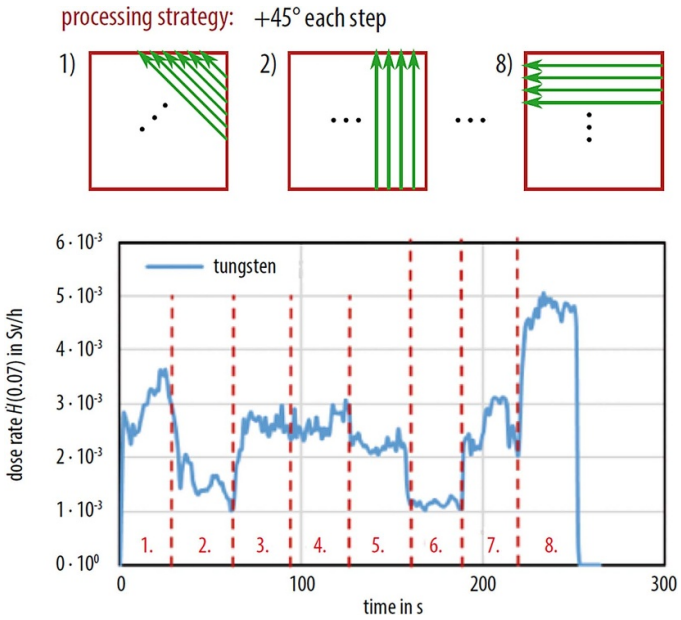

Figure 6. Dose rate $\dot{H}'(0.07)$ recorded during different laser processing steps as function of the processing time [17]. The OD-02 dosimeter was placed at a distance of 200 mm from the interaction zone. The processed material was tungsten. A hatching pattern was rotated by 45° every 31 s, as shown in the upper insert. Each of the individual processing steps is marked by a red number and separated by vertical red dotted lines. The average laser power was 35 W, the repetition rate 200 kHz, the pulse energy 174 μJ and the focal spot diameter 10 μm. This results in a maximum intensity at the focus of 4.7×10^{14} W cm^{-2}. Freitag C and Giedl-Wagner R 2020 X-ray protection in an industrial production environment *Photonics Views* **17** 37–41. Copyright Wiley-VCH GmbH. Reproduced with permission.

above 30 keV. For practical use an equivalent shielding thickness of different materials for attenuation up to 60 keV was conservatively estimated 'in units of iron' as shown in table 1. The value for aluminium had been calculated too strictly in [16] and is corrected to 22 mm here.

Another important aspect that has to be considered is the directional dependence of the emitted x-ray field in laser material processing. In contrast to x-ray tubes, the main direction of the emission, its strength and its spectral distribution can change continuously during the machining process and is essentially determined by the local surface topography at the laser processing spot. The latter is demonstrated in figure 6.

Since the strength of the emitted radiation field also depends on the angle of incidence of the laser beam on the local surface, a constant primary radiation field cannot be expected in radiation protection measurement during laser material processing. This fact complicates the finding of an adequate shielding, especially if the machining process is flexible. In addition, many laser systems allow the change of laser parameters, such as laser pulse energy, pulse duration, laser wavelength and repetition rate. Consequently, the spectral distribution and strength of the x-ray radiation field varies. Furthermore, the laser intensity and therefore the spectral distribution of the emitted x-ray radiation field depend on the focusing optics used. Considering all these factors influencing the x-ray radiation field a worst-case scenario must be assumed in shielding estimations, which takes into account all imaginable machining procedures, workpieces and adjustable laser parameters. However, in industrial mass production with fixed processing parameters and laser settings, the optimized production process itself can be considered as worst-case scenario.

5.2. Method for calculation of a radiation shielding

In order to calculate a suitable shielding, the spectral x-ray emission generated during the machining process must be known. In order to cover the greatest possible risk potential, the worst-case scenario must be assumed which can also be an industrial mass production process. If no machining process can be defined, the worst case must be determined within the scope of a risk analysis reflecting a process with the highest risk potential for all adjustable parameters [12].

From a measured x-ray spectrum, the spectral photon flux can be calculated. Conversion factors provided by ICRU and ICRP [44] or other sources [45] can be used to calculate a spectral dose rate from the spectral photon flux. Integration over the spectral dose rate yields the overall dose rate emitted by the radiation source, which can be confirmed by simultaneously performed dose rate measurements using a dosimeter suitable for pulsed radiation. The dose rate behind a shielding material with proper thickness can be estimated in the same way by integrating the product of spectral dose rate and energy dependent transmission of the shielding material (for more details refer to [12, 16]).

6. Summary

The unwanted emission of x-ray radiation during ultra-short pulse laser processing of materials at air is reviewed. Due to high laser pulse repetition rates, low single pulse x-ray doses can accumulate to harmful skin or effective x-ray doses. Radiation protection strategies are needed in modern laser machining facilities.

Acknowledgments

The authors gratefully acknowledge financial support by the German Federal Ministry of Education and Research (BMBF) in the funding program Photonics Research Germany under contract number 13N14249 and the Federal Office for Radiation Protection (BfS) for the support under the administrative agreement with contract number 3619S22370.

ORCID iDs

Herbert Legall https://orcid.org/0000-0002-2043-0417

Jörn Bonse https://orcid.org/0000-0003-4984-3896
Jörg Krüger https://orcid.org/0000-0003-2632-9448

References

[1] Bäuerle D 2011 *Laser Processing and Chemistry* 4th edn (Berlin: Springer)
[2] Giesen A, Hügel H, Voss A, Wittig K, Brauch U and Opower H 1994 *Appl. Phys.* B **58** 365
[3] Russbueldt P, Mans T, Rotarius G, Weitenberg J, Hoffmann H and Poprawe R 2009 *Opt. Express* **17** 12230
[4] Hädrich S *et al* 2016 *Opt. Lett.* **41** 4332
[5] Kühlke D, Herpers U and von der Linde D 1987 *Appl. Phys. Lett.* **50** 1785
[6] Stearns D G, Landen O L, Campbell E M and Scofield J H 1988 *Phys. Rev.* A **37** 1684
[7] Harris S E and Kmetec J D 1988 *Phys. Rev. Lett.* **61** 62
[8] Zigler A, Burkhalter P G, Nagel D J, Boyer K, Luk T S, McPherson A, Solem J C and Rhodes C K 1991 *Appl. Phys. Lett.* **59** 777
[9] Murnane M M, Kapteyn H C, Rosen M D and Falcone R W 1991 *Science* **251** 531
[10] Thogersen J, Borowiec A, Haugen H K, McNeill F E and Stronach I M 2001 *Appl. Phys.* A **73** 361
[11] Bunte J, Barcikowski S, Püster T, Burmester T, Brose M and Ludwig T 2004 *Top. Appl. Phys.* **96** 309
[12] Legall H, Schwanke C, Pentzien S, Dittmar G, Bonse J and Krüger J 2018 *Appl. Phys.* A **124** 407
[13] Behrens R, Pullner B and Reginatto M 2019 *Radiat. Prot. Dosim.* **183** 361
[14] Legall H, Schwanke C, Bonse J and Krüger J 2019 *Appl. Phys.* A **125** 570
[15] Weber R, Giedl-Wagner R, Förster D J, Pauli A, Graf T and Balmer J E 2019 *Appl. Phys.* A **125** 635
[16] Legall H, Schwanke C, Bonse J and Krüger J 2020 *J. Laser Appl.* **32** 022004
[17] Freitag C and Giedl-Wagner R 2020 *Photonics Views* **17** 37
[18] Bonse J and Krüger J 2010 *J. Appl. Phys.* **107** 054902
[19] von der Linde D and Sokolowski-Tinten K 2000 *Appl. Surf. Sci.* **154–155** 1
[20] Eberle G, Dold C and Wegener K 2015 *Int. J. Adv. Manuf. Technol.* **81** 1117
[21] Saraceno C J, Sutter D, Metzger T and Abdou Ahmed M 2019 *J. Eur. Opt. Soc.* **15** 15
[22] Gillner A, Finger J, Gretzki P, Niessen M, Bartels T and Reininghaus M 2019 *J. Laser Micro Nanoeng.* **14** 129
[23] Loeschner U, Schille J, Streek A, Knebel T, Hartwig L, Hillmann R and Endisch C 2015 *J. Laser Appl.* **27** S29303
[24] International Commission on Radiological Protection 1991 1990 Recommendations of international commission on radiological protection Publication No. 60 (Oxford and New York, Pergamon) *Ann. ICRP* **21** 1–201
[25] Ankerhold U, Hupe O and Ambrosi P 2009 *Radiat. Prot. Dosim.* **135** 149
[26] Ambrosi P, Borowski M and Iwatschenko M 2010 *Radiat. Prot. Dosim.* **139** 483
[27] Hupe O, Zutz H and Klammer J 2012 *IRPA 2012 conf.* Glasgow (available at: www.irpa.net/members/TS2f.3.pdf)
[28] Otto T 2016 *Radiat. Prot. Dosim.* **168** 1
[29] Curcio A, Andreoli P, Cipriani M, Claps G, Consoli F, Cristofari G, De Angelis R, Giulietti D, Ingenito F and Pacella D 2016 *J. Instrum.* **11** C05011
[30] Legall H *et al* 2009 *J. Appl. Crystallogr.* **42** 572
[31] Gerlach M, Anklamm L, Antonov A, Grigorieva I, Holfelder I, Kanngießer B, Legall H, Malzer W, Schlesiger C and Beckhoff B 2015 *J. Appl. Crystallogr.* **48** 1381
[32] Gruner S M, Eikenberry E F and Tate M W 2006 Comparison of X-ray detectors *International Tables for Crystallography, Volume F: Crystallography of Biological Macromolecules*, ed M G Rossmann and E Arnold (Berlin: Springer)
[33] Behrens R, Schwoerer H, Düsterer S, Ambrosi P, Pretzler G, Karsch S and Sauerbrey R 2003 *Rev. Sci. Instrum.* **74** 961
[34] Giulietti D and Gizzi L A 1998 *Riv. Nuovo Cim.* **21** 1
[35] Chen F F 1974 *Introduction to Plasma Physics* (New York: Plenum)
[36] Attwood D 2007 *Soft X-Rays and Extreme Ultraviolet Radiation: Principles and Applications* (Cambridge: Cambridge University Press)
[37] Kruer W L 1988 *The Physics of Laser Plasma Interactions* (California: Addison-Wesley)
[38] Eliezer S 2002 *The Interaction of High-Power Lasers with Plasmas* (Bristol: IOP Publishing)

[39] Gibbon P 2005 *Short Pulse Laser Interaction with Matter* (London: Imperial College Press)
[40] Chichkov B N, Momma C, Tünnermann A, Meyer S, Menzel T and Wellegehausen B 1996 *Appl. Phys. Lett.* **68** 2804
[41] Forslund D W, Kindel J M and Lee K 1977 *Phys. Rev. Lett.* **39** 284
[42] Krol A, Ikhlef A, Kieffer J C, Bassano D A, Chamberlain C C, Jiang Z, Pépin H and Prasad S C 1997 *Med. Phys.* **24** 725
[43] Kieffer J C, Krol A, Jiang Z, Chamberlain C C, Scalzetti E and Ichalalene Z 2002 *Appl. Phys.* B **74** 75
[44] International Commission on Radiological Protection 2010 Conversion coefficients for radiological protection for external radiation exposures ICRP Publication 116 (Oxford, Elsevier Science) *Ann. ICRP* **40** 1–257
[45] Veinot K G and Hertel N E 2011 *Radiat. Prot. Dosim.* **145** 28